Tests of quantum-gravity-induced nonlocality
via optomechanical experiments

Alessio Belenchia,[1,2,*] Dionigi M. T. Benincasa,[1,†] Stefano Liberati,[1,‡] Francesco Marin,[3,4,§]
Francesco Marino,[5,‖] and Antonello Ortolan[6,¶]

[1]*SISSA, Via Bonomea 265, I-34136 Trieste, Italy and INFN, Sez. di Trieste*
[2]*CNR-Istituto Nazionale di Ottica, Largo E. Fermi 6, I-50125 Firenze, Italy*
[3]*Dipartimento di Fisica e Astronomia, University of Florence, Via Sansone 1,*
I-50019 Sesto Fiorentino, Firenze, Italy and INFN, Sez. di Firenze
[4]*European Laboratory for Non-Linear Spectroscopy (LENS), Via Carrara 1,*
I-50019 Sesto Fiorentino, Firenze, Italy
[5]*CNR-Istituto Nazionale di Ottica, Largo E. Fermi 6, I-50125 Firenze, Italy and INFN, Sez. di Firenze*
[6]*INFN, Laboratori Nazionali di Legnaro, Viale dell'Università, 2, 35020 Legnaro, Padova, Italy*

The nonrelativistic limit of nonlocal modifications to the Klein-Gordon operator is studied, and the experimental possibilities of casting stringent constraints on the nonlocality scale via planned and/or current optomechanical experiments are discussed. Details of the perturbative analysis and semianalytical simulations leading to the dynamic evolution of a quantum harmonic oscillator in the presence of nonlocality reported in [A. Belenchia, D. M. T. Benincasa, S. Liberati, F. Marin, F. Marino, and A. Ortolan, Phys. Rev. Lett. **116**, 161303 (2016)] are given, together with a comprehensive account of the experimental methodology with particular regard to sensitivity limitations related to thermal decoherence time and active cooling of the oscillator. Finally, a strategy for detecting nonlocality scales of the order of $10^{-22} \div 10^{-26}$ m by means of the spontaneous time-periodic squeezing of quantum-coherent states is provided.

I. INTRODUCTION

Quantum gravity phenomenology is the phrase commonly used to describe the field of research that attempts to build a bridge between Planck-scale theories of quantum gravity (QG) and observation. The real challenge faced by the community working in this field is to derive phenomenology that is relevant at scales much lower than the Planck scale, $M_p = 1.22 \times 10^{28}$ eV, where QG effects are expected to dominate, so that existing models can be put to the test. Over the last two decades there has been a steady stream of work in this direction. In particular, relevant studies include tests of quantum decoherence and state-collapse models [1], QG imprints on initial cosmological perturbations [2], cosmological variation of coupling constants [3,4], TeV Black Holes within extradimensions [5], Planck-scale spacetime fuzziness [6], generalized uncertainty principles [7–9], violations of discrete symmetries [10], and violations of spacetime symmetries [11,12]. In this paper we add to this list by considering the phenomenological effects of a fundamental "spacetime nonlocality" in nonrelativistic, macroscopic quantum systems.

The underlying idea here is that models of QG with fundamental Lorentz invariance (LI) lead to low-energy effective theories with dynamics that are nonlocal in spacetime once the high-energy degrees of freedom have been integrated out. Particular examples of this kind exist in causal set theory, where the interplay between Lorentz invariance and discreteness leads to nonlocal dynamics for fields living on the causal set [13]; string theory and string field theory where the string and its interactions are inherently nonlocal [14]; and noncommutative geometry [15].[1] It therefore appears that, in general, theories of QG in which continuum spacetime emerges from more fundamental constituents and where LI is preserved can only be realized at the expense of modifying low-energy effective dynamics in an essentially nonlocal way.

To be more specific, let us consider a free massive scalar field, ϕ, on a flat spacetime that has "emerged" from a LI theory of QG. The most naïve thing that one can imagine is that the emerging field theory is just a standard local field theory described by the equations of motion $(\Box + m^2)\phi(x) = 0$. A little more thought, however, reveals that this is unlikely to be the case. Indeed any theory of QG gravity must at the very least contain the scale $l_p = 1.62 \times 10^{-35}$ m; therefore, following the usual ideas

[*]abelen@sissa.it
[†]dionigi.benincasa@sissa.it
[‡]liberati@sissa.it
[§]marin@fi.infn.it
[‖]marino@fi.infn.it
[¶]antonello.ortolan@lnl.infn.it

---

[1]It has also been argued that the same form of nonlocality must also be present in loop quantum gravity if it has any hope of preserving LI [16].

of effective field theory (EFT), it is natural to expect this scale to enter the low-energy physics as a perturbative parameter in an expansion around the local theories we know and love. Thus, combining this with the fact that the theory is fundamentally LI, the most natural dynamics that one might write down for such a field theory is something like $f(\Box + m^2)\phi = 0$, where f is some nonpolynomial function of the Klein-Gordon (KG) operator such that $f(\Box + m^2) \rightarrow \Box + m^2$ in the limit $l_p \rightarrow 0$.[2] In a sense one can think of f as providing the UV completion of the EFT.

It should come as no surprise then that this is precisely what one finds in the models referred to above. For example, in four dimensions string field theory predicts a nonlocal KG equation of the form [18]

$$f(\Box + m^2) = (\Box + m^2)\exp[l_p^2(\Box + m^2)], \quad (1)$$

while causal set theory gives[3]

$$f(\Box + m^2) = (\Box + m^2) - \frac{3l_p^2}{2\pi\sqrt{6}}(\Box + m^2)^2$$

$$\times \left[3\gamma - 2 + \ln\left(\frac{3l_p^2(\Box + m^2)^2}{2\pi}\right)\right] + \ldots,$$

$$(2)$$

where γ is Euler-Mascheroni's constant. Note that in the first instance the function f is an *analytic* function, while in the second it is *nonanalytic*. Further it turns out that the scale entering the definition of f need not be identified with the Planck scale itself in general. This happens, for example, with causal set d'Alembertians, where theoretical considerations have led Sorkin to postulate that the scale entering their definition is some $l_k \gg l_p$ [13]. This is crucial for phenomenology since there is little hope in detecting nonlocal effects if they only become relevant at the Planck scale. From here on we will therefore take the nonlocality scale l_k to be a free parameter of the theory.

In the rest of this paper we will explore a new phenomenological approach based on the application of the nonrelativistic limit of an analytic nonlocal KG equation [e.g., (1)] to optomechanical quantum oscillators.[4] We will argue that the true evolution of this system is governed by a nonlocal Schrödinger equation whose specific form depends on the underlying nonlocal relativistic Quantum Field Theory (QFT). Finally we will analyze in perturbation

theory the effects induced by the lowest order corrections to the standard Schrödinger evolution.

The paper is organized as follows. In Sec. II we discuss the nonrelativistic limit of nonlocal relativistic QFTs characterized by analytic form factors f. In particular, we will discuss the properties that a nonlocal QFT must possess in order for there to exist a sensible physical interpretation of its nonrelativistic limit. Section III describes the perturbative analysis of the nonlocal Schrödinger equation in the presence of an external potential. In Sec. IV we apply this analysis to the specific case of a harmonic oscillator potential, thus reproducing the results reported in [21] with a greater level of detail. Finally, in Sec. V we discuss in detail the experimental strategies that can be used to cast limits on the nonlocality scale with current, and near future, experiments involving macroscopic quantum oscillators. Conclusions and a discussion of future work are given in Sec. VI.

II. NONRELATIVISTIC LIMIT OF NONLOCAL RELATIVISTIC QFTS

Consider a free complex, massive, scalar nonlocal QFT defined by the Lagrangian

$$\mathcal{L} = \phi(x)^* f(\Box + \mu^2)\phi(x) + \text{c.c.,} \quad (3)$$

where $\Box = c^{-2}\partial_t^2 - \nabla^2$ and $\mu = mc/\hbar$. In order for the theory to be physically sensible, we assume that the following conditions hold:

(1) $f(k^2) = 0$ iff $k^2 = 0$: This property ensures that there exist no classical runaway solutions and, when f is entire, no ghosts.

(2) The nonlocal QFT must be unitary: conservation of probability.

(3) The nonlocal QFT must possess a global $U(1)$ symmetry: this condition ensures that (some form of) a probabilistic interpretation can be given to the wave function.

As already mentioned, the function f can be both entire analytic and nonanalytic. For the remainder of this paper we will assume that f is entire analytic so that it can be expanded as

$$f(z) = \sum_{n=1}^{\infty} b_n z^n. \quad (4)$$

Implicit in the definition of f is the nonlocality scale l_k which, in the local limit $l_k \rightarrow 0$, sends $f(\Box + \mu^2) \rightarrow \Box + \mu^2$. In particular, we have that $b_n \propto l_k^{2n-2}$ and $b_1 = 1$.

Following standard treatments (see, e.g., Sec. 2.8 of [22]) we decompose the field as $\phi(x) = e^{-i\frac{mc^2}{\hbar}t}\psi(t, \boldsymbol{x})$. Substituting this into our Lagrangian and taking the limit $c \rightarrow \infty$ we find

---

[2]The infinite number of derivatives is crucial in order to avoid Ostrogradski's theorem [17], which also applies to theories with higher order, but finite, powers of the d'Alembertian operator $\Box$.

[3]Note that $f(\Box + m^2)$ was rigorously derived from causet theory only in the case $m = 0$, but see discussion in [19] on ways of extending this to the massive case.

[4]We will not discuss the phenomenology of nonanalytic nonlocal QFTs here, but for recent ideas on this we refer the reader to [20]

$$\mathcal{L}_{\mathrm{NR}} = \psi^*(t, \boldsymbol{x}) f(\mathcal{S}') \psi(t, \boldsymbol{x}) + \mathrm{c.c.}, \qquad (5)$$

where NR stands for nonrelativistic, $\mathcal{S}' = -\frac{2m}{\hbar^2}\mathcal{S}$, and

$$\mathcal{S} = i\hbar \frac{\partial}{\partial t} + \frac{\hbar^2}{2m}\nabla^2 \qquad (6)$$

is the Schrödinger operator.

To derive the equations of motion, we use a nonlocal generalization of the Euler-Lagrange equations [23], which gives

$$f(\mathcal{S})\psi(t, \mathbf{x}) = 0, \qquad (7)$$

where

$$f(\mathcal{S}) \equiv \frac{-\hbar^2}{2m} f(\mathcal{S}') = \mathcal{S} + \sum_{n=2}^{\infty} b_n \left(\frac{-2m}{\hbar^2}\right)^{n-1} \mathcal{S}^n. \quad (8)$$

One can also include an external potential, $V(x)$, by adding the term $V(x)\psi^*\psi$ to the Lagrangian (5). To simplify notation we set $b_n = l_k^{2n-2} a_n$ so that equation (8) becomes

$$f(\mathcal{S}) = \sum_{n=1}^{\infty} (-2m/\hbar^2)^{n-1} a_n l_k^{2n-2} \mathcal{S}^n. \qquad (9)$$

The Lagrangian (5) possesses a global $U(1)$ symmetry $\psi \to e^{i\alpha}\psi$ whose conserved current, j_{NL}^{μ}, can be shown to be given by

$$\begin{aligned} j_{NL}^0 = {}& a_1 \psi^*\psi - ia_2 l_k^2 \frac{2m}{\hbar} \psi^* \overset{\leftrightarrow}{\partial_t} \psi - a_2 l_k^2 \psi^* \nabla^2 \psi \\ & - a_2 l_k^2 \psi \nabla^2 \psi^* + O(l_k^4) \end{aligned} \qquad (10)$$

$$\begin{aligned} j_{NL}^i = {}& -ia_1 \frac{\hbar}{2m} \psi^* \overset{\leftrightarrow}{\nabla} \psi + ia_2 l_k^2 \frac{\hbar}{2m} \psi^* \overset{\leftrightarrow}{\nabla^3} \psi \\ & + 2a_2 l_k^2 \dot{\psi}^* \overset{\leftrightarrow}{\nabla} \psi + O(l_k^4), \end{aligned} \qquad (11)$$

where $f \overset{\leftrightarrow}{\nabla}^n g = \sum_{i=0}^{n}(-)^i \nabla^i f \nabla^{n-i} g$. Note that, as required by consistency with the local theory,

$$(j_{NL}^0, j_{NL}^i) \to \left(\psi^*\psi, -ia_1 \frac{\hbar}{2m} \psi^* \overset{\leftrightarrow}{\nabla} \psi\right) \qquad (12)$$

as $l_k \to 0$.

What we have so far is a nonrelativistic field ψ satisfying a nonlocal generalization of the Schrödinger equation. What we want though is to be able to interpret ψ as the wave function of a quantum mechanical system. The canonical way of doing this in the local theory is to define a one-particle wave function for a generic one-particle state constructed from the field operator ψ and show that this wave function satisfies the same Schrödinger equation as

the field. This analysis requires the Hamiltonian, which we currently lack in our nonlocal theory. Thus, from here on we will proceed with the caveat that our model is only phenomenological in the sense that we have yet to demonstrate that the one-particle wave function of the nonrelativistic field satisfies the nonlocal Schrödinger equation. We will comment more on this in the conclusions.

III. PERTURBATIVE ANALYSIS

Having laid down the foundations for a nonlocal Schrödinger evolution of a single-particle quantum system, we now turn to the problem of solving the nonlocal differential equation in the presence of a time-independent potential $V(x)$.

We wish to solve the nonlocal equation

$$f(\mathcal{S})\psi(t, x) = V(x)\psi(t, x), \qquad (13)$$

where $f(\mathcal{S})$ is some analytic function as in (9), and $V(x)$ is some physically reasonable binding potential. Since the above equation is extremely hard to solve exactly for a given nontrivial potential V, we will solve it *perturbatively*.

In order to cast (13) in a form amenable to a perturbative analysis, we first note that the presence of an external binding potential $V(x)$ introduces an energy scale that can be parametrized as $\hbar\omega$, where the "scale" ω has dimensions of $(\mathrm{time})^{-1}$. We can use this new scale, together with the other scales in the problem, to construct a dimensionless parameter $\epsilon \coloneqq m\omega l_k^2/\hbar$. For physically reasonable choices m, ω, and l_k, ϵ is much smaller than unity, so we can use it as our perturbative parameter in the expansion of $f(\mathcal{S})$

$$f(\mathcal{S}) = \mathcal{S} - \frac{2a_2}{\hbar\omega}\epsilon\mathcal{S}^2 + \sum_{n=3}^{\infty} a_n \left(\frac{-2}{\hbar\omega}\right)^{n-1} \epsilon^{n-1}\mathcal{S}^n. \quad (14)$$

Next, we will assume that (14) admits solutions of the form

$$\psi = \sum_{n=0}^{\infty} \epsilon^n \psi_n. \qquad (15)$$

Substituting (15) into (14), we find the following set of differential equations:

$$O(1): (\mathcal{S} - V)\psi_0 = 0, \qquad (16)$$

$$O(\epsilon): (\mathcal{S} - V)\psi_1 = J_1, \qquad (17)$$

$$O(\epsilon^2): (\mathcal{S} - V)\psi_2 = J_2,$$
$$\mathrm{etc.,} \qquad (18)$$

where the J_i, $i = 1, 2, \ldots$ are source terms. Note that the ith source term depends on the solution to the $(i-1)$th order problem, for example,

$$J_1 = \frac{2a_2}{\hbar\omega} \mathcal{S}^2 \psi_0, \qquad (19)$$

$$J_2 = \frac{-4a_3}{\hbar^2\omega^2} \mathcal{S}^3 \psi_1, \quad \text{etc.} \qquad (20)$$

Implicit in the above analysis is the assumption that ψ_0, a solution to the standard Schrödinger equation, is also an approximate solution to the nonlocal equation, i.e., that

$$|(f(\mathcal{S}) - V)\psi_0| = O(\epsilon) \ll 1, \quad \forall \, t, x. \qquad (21)$$

The idea behind this assumption is that nonlocal extensions, f, of experimentally verified local models must be such that they admit solutions to the local models as approximate solutions. Clearly this assumption is difficult to check explicitly, especially here where we have a function of the operator $\mathcal{S}$ containing both space and time derivatives.

We can summarize our perturbative approach as follows:
(1) Consider nonlocal Schrödinger equations with entire analytic $f(\mathcal{S})$ s in the presence of an external potential $V(x)$ that satisfy (21).
(2) Using the scale introduced by the potential, construct a (small) dimensionless parameter ϵ.
(3) Expand $f(\mathcal{S})$ in ϵ and assume that solutions can be written as (15).
(4) Solve the problem order by order in ϵ, checking that the conditions are satisfied at each order.
(5) Finally, one should check for consistency that each term $\epsilon^n \psi^n$ is indeed smaller than the previous one, $\epsilon^{n-1} \psi^{n-1}$, for each n (up to the relevant order of interest).

IV. NONLOCAL SCHRÖDINGER EQUATION IN $(1+1)$D WITH A HARMONIC OSCILLATOR POTENTIAL

Consider a single particle in a harmonic oscillator potential in $1+1$ dimensions satisfying the equation

$$f(\mathcal{S})\psi(t, x) = \frac{1}{2} m\omega^2 x^2 \psi(t, x), \qquad (22)$$

where m is the mass of the system and ω its angular frequency. Following the steps laid out in the previous section, we construct the dimensionless parameter $\epsilon \equiv m\omega l_k^2/\hbar$ and write $f(\mathcal{S})$ as

$$\left(\mathcal{S} - \frac{2a_2}{\hbar\omega} \epsilon \mathcal{S}^2 + \sum_{n=3}^{\infty} a_n \left(\frac{-2}{\hbar\omega} \right)^{n-1} \epsilon^{n-1} \mathcal{S}^n \right) \psi(t, x)$$

$$= \frac{1}{2} m\omega x^2 \psi(t, x). \qquad (23)$$

In order to keep the notation as clear as possible, we define the following dimensionless variables $\hat{t} = \omega t$,

$\hat{x} = \sqrt{\omega m/\hbar} x$, and $\hat{\psi} = \gamma\psi$, where γ has dimensions of $1/\sqrt{\text{Length}}$, so that (23) becomes

$$\left(\hat{\mathcal{S}} - 2a_2 \epsilon \hat{\mathcal{S}}^2 + \sum_{n=3}^{\infty} a_n \epsilon^{n-1} (-2)^{n-1} \hat{\mathcal{S}}^n \right) \hat{\psi} = \frac{1}{2} \hat{x}^2 \hat{\psi}. \qquad (24)$$

Throughout the rest of this section we will use these dimensionless variables but will drop the hat symbol for notational simplicity.

We assume that (23) admits solutions of the form (15). In particular, we will be interested in solutions that are perturbations around the coherent state

$$\psi_0 := \psi_\alpha(t, x)$$

$$= \frac{1}{\pi^{1/4}} \exp\left[\sqrt{2}\alpha e^{-it} x - \frac{1}{2}\alpha^2 e^{-2it} - \frac{\alpha^2}{2} - \frac{it}{2} - \frac{x^2}{2} \right], \qquad (25)$$

where without loss of generality α can be taken as real and $(\mathcal{S} - x^2/2)\psi_0 = 0$. This choice of ψ_0 is motivated by the fact that coherent states are relatively easy to realize within the experimental setting we have in mind (see Sec. V) and furthermore include the harmonic oscillator's ground state as a specific case.

Next, we want to solve the differential equation at order ϵ. To this end we first substitute ψ_0 into (19) to find

$$J_1 = a_2 \frac{1}{2\pi^{1/4}} e^{-\frac{1}{2} e^{-2it}(-2\sqrt{2} e^{it} x\alpha + \alpha^2 + e^{2it}(3it+x^2+\alpha^2))}$$

$$\times (e^{it}(2 - 4x^2 + x^4) + 4\sqrt{2}x\alpha). \qquad (26)$$

Then, to solve $(\mathcal{S} - V)\psi_1 = J_1$ we use the ansatz

$$\psi_1(t, x) = \psi_0(t, x)[c_0(t) + c_1(t)x + c_2(t)x^2 + c_3(t)x^3 + c_4(t)x^4], \qquad (27)$$

which leads to the following system of ordinary differential equations for the time-dependent coefficients $c_i(t)$:

$$0 = 2i\dot{c}_4(t) - 8c_4(t) - a_2,$$
$$0 = ie^{it}\dot{c}_3(t) - 3e^{it}c_3(t) + 4\sqrt{2}\alpha c_4(t),$$
$$0 = e^{it}(i\dot{c}_2(t) + 6c_4(t) + 2a_2) - 2e^{it}c_2(t) + 3\sqrt{2}\alpha c_3(t),$$
$$0 = \sqrt{2}\alpha c_1(t) + e^{it}(i\dot{c}_0(t) + c_2(t) - a_2),$$
$$0 = 4ie^{7it}\dot{c}_1(t) - 4e^{7it}c_1(t)$$
$$\quad - \sqrt{2}\alpha a_2(-3\alpha^2 + 6(2\alpha^2 + 1)e^{2it}$$
$$\quad + e^{4it}(-4 + \alpha^2(-9 + 12it)) + 6e^{6it}), \qquad (28)$$

which we solve using Mathematica 11 subject to the initial condition $\psi_1(0, x) = 0$. Solutions to (28) with the given initial condition contain secular terms which grow linearly

in time as ϵt. These terms are a well-known artifact due to the nonuniform convergence of the perturbative expansion. To avoid the appearance of secular terms, we used the method of multiple scales and refer the reader to Appendix A for further details.

Finally, we find

$$c_0(t) = \frac{1}{32} a_2 e^{-8it} (\alpha^4 - 8\alpha^4 e^{2it} + 8\alpha^4 e^{6it} - \alpha^4 e^{8it}$$
$$- 6\alpha^2 e^{2it} + 20\alpha^2 e^{4it} - 14\alpha^2 e^{6it} + 28\alpha^2 e^{8it}$$
$$- 3e^{4it} - 4e^{6it} + 7e^{8it}), \tag{29}$$

$$c_1(t) = -\frac{1}{4\sqrt{2}} \alpha a_2 e^{-7it} (\alpha^2 - 6\alpha^2 e^{2it} + 3\alpha^2 e^{4it}$$
$$+ 2\alpha^2 e^{6it} - 3e^{2it} + 4e^{4it} - e^{6it}), \tag{30}$$

$$c_2(t) = \frac{1}{8} a_2 e^{-6it} (3\alpha^2 - 12\alpha^2 e^{2it} + 9\alpha^2 e^{4it}$$
$$- 3e^{2it} - 2e^{4it} + 5e^{6it}), \tag{31}$$

$$c_3(t) = -\frac{1}{2\sqrt{2}} \alpha a_2 e^{-5it} (1 - e^{2it})^2, \tag{32}$$

$$c_4(t) = \frac{1}{8} a_2 e^{-4it} (1 - e^{4it}). \tag{33}$$

Although we do not show it here, the same procedure, including an ansatz similar to Eq. (27) but with a polynomial of order 8, can be used to solve the nonlocal Schrödinger equation to second order in ϵ.

A. Wave function normalization

With the first-order perturbative solution to Eq. (23) at hand, we can now compute expectation values and variances of physical observables in this state. However, for these to make sense we need to first ensure that a probabilistic interpretation of the wave function exists. This requires, at the very least, that the following condition $\int_{-\infty}^{\infty} dx |\psi(x)|^2 = 1$ holds. Now, recall that the conserved charge in Eq. (10) is not simply $|\psi|^2$, so expectation values directly computed using $|\psi_0 + \epsilon \psi_1|^2$ cannot have a well-defined probabilistic interpretation at order ϵ. A quick fix to this problem that leads to a well-defined conserved probability distribution (at least to this order in ϵ) is to normalize the wave function $\psi_0 + \epsilon \psi_1$ using its own norm. In accordance with the Born rule the probability density is then given by

$$\rho(t, x) = \frac{\psi^*(t, x)\psi(t, x)}{\int_{-\infty}^{\infty} |\psi|^2 dx}, \tag{34}$$

so that $\int_{-\infty}^{\infty} dx \rho(x) = 1$ by construction and is therefore conserved. It should be noted that the normalization factor

is 1 at order ϵ when considering perturbations around the ground state, i.e., $\langle \psi_0 | \psi_1 \rangle = 0$, while in the case of a generic coherent state an order ϵ time-dependent correction is present. The above normalization factor ensures that even in this case we a have a meaningful probability distribution.

B. Phenomenology

Given the probability distribution (34), we can compute the mean and variance of the position and momentum of the particle. We find

$$\langle x \rangle = \sqrt{2}\alpha \cos(t) \left(1 + \frac{1}{4} \epsilon \alpha^2 a_2 [\cos(2t) - 1] \right) + \mathcal{O}(\epsilon^2), \tag{35}$$

$$\langle p \rangle = \sqrt{2}\alpha \sin(t) \left(1 + \frac{1}{4} \epsilon a_2 [\alpha^2 (7 + 3\cos(2t)) - 2] \right)$$
$$+ \mathcal{O}(\epsilon^2), \tag{36}$$

$$\text{Var}(x) = \frac{1}{2} (1 - \epsilon a_2 [(6\alpha^2 - 1)\sin^2(t)]) + \mathcal{O}(\epsilon^2), \tag{37}$$

$$\text{Var}(p) = \frac{1}{2} (1 + \epsilon a_2 [(6\alpha^2 - 1)\sin^2(t)]) + \mathcal{O}(\epsilon^2). \tag{38}$$

Therefore, on the basis of Eqs. (35)–(38), the effects of nonlocality appear in the form of deviations from the standard variances and mean values of position and momentum, as shown in Figs. 1 and 2. In particular, our model predicts an oscillatory behavior of the variance of x, together with a time-averaged expectation value that is larger than the standard $x_{\text{zpm}}^2 = \hbar/2m\omega$, and a third-harmonic distortion in the evolution of coherent states.

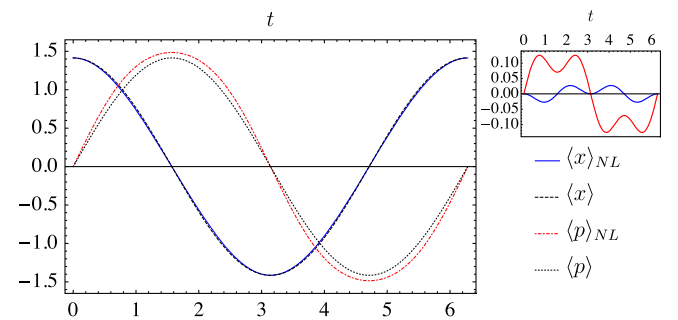

FIG. 1. Periodic time dependence of the mean position and momentum for a coherent state for $\alpha = 1$, $a_2 = 1$, and we have set $\epsilon = 10^{-1}$ to amplify the effect of the nonlocality. The continuous blue and red lines represent the mean position and momentum in Eqs. (35) and (36), respectively. The black dotted and black dashed lines represent the mean position and momentum for the standard coherent state, respectively. The insert on the top right shows the order ϵ corrections to the standard coherent state for the mean position (blue) and momentum (red).
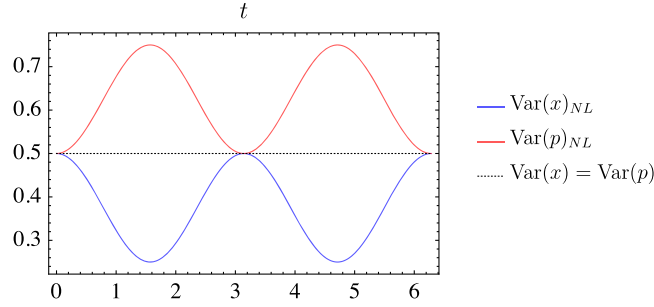
FIG. 2.   Periodic time dependence of the variances of position and momentum for a coherent state for $\alpha = 1$, $a_2 = 1$, and $\epsilon = 10^{-1}$. The continuous blue and red lines represent the variance of position and momentum in Eqs. (37) and (38), respectively. The black dotted line represents the variance of position and momentum for the standard coherent state, which is equal to $1/2$.

The strength of these effects is governed by the perturbation parameter ϵ.

Let us remark that $\sqrt{\epsilon}$ is given by the ratio between l_k and the size of the ground-state wave packet $x_{\text{zpm}} = \sqrt{\hbar/2m\omega}$, i.e., the zero-point fluctuations. Such dependence suggests that massive quantum systems or, more precisely, systems with the smallest zero-point fluctuations, could be the ideal setting for detecting such nonlocality. Furthermore, $\text{Var}(x)\text{Var}(p) = 1/4 + O(\epsilon^2)$, so the perturbed state is still a state of minimum uncertainty but one which undergoes a spontaneous, cyclic, time-dependent "squeezing" in position and momenta (see Fig. 2). The word squeezing is apt in view of the fact that the state is one of minimum uncertainty.

Finally, it is worth noting that the expectation values of x and p in the ground state ($\alpha = 0$) are identical to the standard local case to first order in ϵ (and indeed the same holds true to second order), while the variances are always modified to order ϵ, except for the peculiar case $\alpha = \pm 1/\sqrt{6}$. This peculiarity appears to be a numerical accident—as is confirmed by going to order ϵ^2 where the values $\alpha = \pm 1/\sqrt{6}$ play no special role—so we attach no particular physical meaning to it.

C. Range of validity of the perturbative expansion

Before we proceed, an important point to make is that the validity of the perturbative expansion depends on the state that we choose to expand around. In this case, expanding around the coherent state (25) implies that the validity of the expansion will also depend on α. To see this, consider the L_2 distance between ψ_0 and ψ to first order in ϵ,

$$\|\psi_0 - (\psi_0 + \epsilon\psi_1)\| \propto \epsilon|\alpha|^4.$$

This tells us that for the perturbative expansion to be valid one must require that $\epsilon\alpha^4 \ll 1$ and not just $\epsilon \ll 1$.
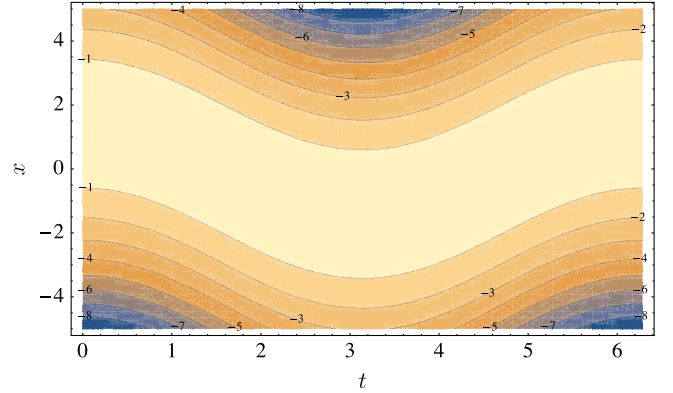

FIG. 3.   A contour plot of $\log_{10}(|\epsilon\psi_1|/|\psi_0|)$ for $\alpha = 1$, $\epsilon = 10^{-3}$, and $a_2 = 1$. Note that although ψ_1 dominates over ψ_0 for large $|x|$ because of the form of our ansatz at spatial infinity, the total wave function is still suppressed by a Gaussian factor. Furthermore, due to the presence of a binding potential, these regions are irrelevant for the experimental system we are modeling. We have also checked the analogous condition for the order ϵ^2 solution with similar results.

Finally, we checked for consistency that $|\epsilon\psi_1|/|\psi_0| \ll 1$ (at least in the spacetime region relevant to the actual systems under consideration), with results shown in Fig. 3.

V. OPTOMECHANICAL TESTS OF NONLOCALITY

In this section we provide a detailed discussion of possible experimental tests of our model using optomechanical experiments based on macroscopic quantum oscillators. For definiteness we will assume that $a_2 = 1$.

Nowadays optomechanical experiments can cool a macroscopic oscillator down to thermal occupation numbers below unity, as well as prepare mechanical squeezed states. In most cases the mechanical system is coupled to an electromagnetic field that is either used to prepare the oscillator in its quantum ground state or to monitor its motion. In these setups the wave function ψ is associated with an effective coordinate describing the displacement of a normal mode, or, to some approximation, to the center-of-mass motion of the mechanical oscillator.

Let us stress that the modeling of optomechanical interactions in the presence of nonlocality is not straightforward and currently is not included in our prototype model. Therefore, limits obtainable from current experiments, while providing preliminary hints on the length scales achievable in optomechanical setups, should not be used for a quantitative comparison with our model. Nevertheless, it is still possible to conceive experimental schemes, based on state-of-the art technologies, that could potentially improve current limits on the nonlocality scale.

It is also worth mentioning that first bounds have already been obtained by comparing nonlocal relativistic EFTs to the 8 TeV LHC data [24], in which the authors find

$l_k \lesssim 10^{-19}$ m. So it would be of great interest to realize independent experiments able to explore new intermediate regimes between the LHC and the Planck scale. In the following we provide first estimates of the limits achievable via optomechanical experiments.

A. Limits from ground-state variance

First constraints on nonlocal effects can be imposed by comparing the measured variance of x with the corresponding predictions for the ground state. Taking the time average of Eq. (37) with $\alpha = 0$ we find that $\mathrm{Var}(x)$ is increased with respect to its standard value by $\epsilon/2$. In order to compare our predictions with experiments we require both an oscillator energy close enough to its standard ground value (namely, with an average occupation number $\langle n \rangle \ll 1$), and a sufficient accuracy, Δ_{meas}, in the measurement of the variance. With these conditions we derive from Eq. (37) an upper limit to ϵ of the form $\epsilon < 2(\langle x^2 \rangle_{\mathrm{meas}}/x_{\mathrm{zpm}}^2 - 1) = 4\Delta_{\mathrm{meas}}$ and thus a bound on the nonlocality scale, $l_k < 2x_{\mathrm{zpm}}\sqrt{\Delta_{\mathrm{meas}}}$.

The cooling of a mechanical oscillator close to the quantum ground state can be achieved by means of ultracryogenic techniques, e.g., by dilution refrigerators, or by active radiation-pressure cooling starting from precooled oscillators. In the first case, the oscillator is naturally in thermal equilibrium with the cryogenic environment, with temperatures typically around a few tens of mK. In these conditions, an average occupation number $\langle n \rangle < 1$ can be obtained for mechanical oscillators with resonant frequencies in the GHz range and thus with very low masses.

Recent experiments have cooled silicon optomechanical crystals, reaching an average phonon occupancy as low as $\langle n \rangle \approx 0.02$, which has been measured by single-phonon-counting techniques using weak optical excitation pulses [25,26]. In these studies a measurement of the variance of x is not provided, but it could be realized, in principle, by observing the phase fluctuations of the field reflected by the cavity in an interferometric setup. The measurement should be performed in a time shorter than the thermal decoherence time $\tau = (Q/\omega)/(1 + \langle n \rangle) \approx (Q/\omega)$. Here, a crucial problem is to achieve the required sensitivity while using a sufficiently weak probe to avoid the quantum backaction of the measurement field. The latter imposes a further limitation on the measurement time, which now should be shorter than $\tau_{BA} = (Q/\omega)/(1 + \langle n_{BA} \rangle)$, where n_{BA} is the number of thermal phonons produced by the backaction (backaction heating).

In the bad-cavity regime and with a probe power corresponding to the standard quantum limit, one basically obtains $\langle n_{BA} \rangle \approx 1$. We thus consider a single measurement time $\tau_{\mathrm{meas}} \sim (Q/\omega)$ and an optical power smaller by a factor of ten (i.e., $\langle n_{BA} \rangle = 0.1$). In these conditions, the signal-to-noise ratio achieved in a single measurement is just 0.1, but the cycle can be repeated several times in order

to reach an accuracy of the order of 1% that is comparable to the reasonably predictable systematic errors in the estimate of the system's parameters.

The experiments in Refs. [25,26] use similar nanomechanical oscillators with resonant frequencies around 5 GHz. A direct measurement of the mass is not provided, but it can be roughly estimated from the dimensions of the moving part of the photonic crystal to be of the order of $m \approx 10^{-15}$ kg. The corresponding zero-point fluctuations are $x_{\mathrm{zpm}} \sim 3$ fm $= 10^{-15}$ m. Assuming an accuracy $\Delta_{\mathrm{meas}} \sim 1\%$, we obtain $l_k < 6 \times 10^{-16}$ m.

We can also consider mechanical oscillators that are actively cooled by radiation pressure starting from cryogenic or ultracryogenic conditions. By means of this technique it is possible to achieve ground-state cooling of oscillators with larger $m\omega$ and then with a lower x_{zpm}. On the other hand, the oscillator is now kept in a dynamic thermal equilibrium with a hot background (corresponding to thermal occupancies $\langle n \rangle \gg 1$) and a cooling bath provided by the optomechanical interaction. As mentioned before, the effects of the radiation-pressure coupling between optical and mechanical degrees of freedom are neglected in our model. Therefore, we cannot provide any prediction on how nonlocal effects will be modified by such interaction. For a meaningful comparison with our model, the measurement of the variance should be realized within a time τ after turning off the cooling laser.

In order to assess the feasibility of such measurements, we consider two recent experiments with actively cooled oscillators: an aluminum membrane coupled to microwave radiation that is used to cool and monitor its motion [27] and a SiN membrane in a high-finesse optical cavity [28]. In the first case the system's parameters are $m = 5 \times 10^{-14}$ kg, $\omega/2\pi = 15$ MHz, corresponding to $x_{\mathrm{zpm}} \simeq 5$ fm, and a quality factor $Q = 1.6 \times 10^6$. The background temperature is $T = 30$ mK, corresponding to an occupation number $\langle n \rangle = 42$, which is then reduced to $\langle n_{\mathrm{eff}} \rangle \sim 0.2$ by active cooling. In the second case, $m = 9 \times 10^{-12}$ kg, $\omega/2\pi = 1.5$ MHz ($x_{\mathrm{zpm}} \simeq 1.2$ fm), $Q = 8 \times 10^6$, $T = 0.36$ K ($\langle n \rangle = 4800$), and $\langle n_{\mathrm{eff}} \rangle \sim 0.2$. Using the above values of $\langle n \rangle$, we obtain respectively $\tau \simeq 0.4$ ms (6000 oscillation periods) and $\tau \simeq 0.18$ ms (270 oscillation periods). Since the measurement time is much shorter than in the previous case, backaction can be neglected here.

If we perform a single measurement with sensitivity corresponding to the standard quantum limit for continuous detection, the signal-to-noise ratio achieved is $1/\langle n \rangle$ (the detection spectral bandwidth is $\langle n \rangle$ times the natural linewidth of the mechanical resonance). In order to achieve an accuracy of around 10%, the measurement should thus be repeated $100\langle n \rangle^2$ times, which can be reasonably done for the oscillator with $\langle n \rangle = 42$. In this case we obtain $l_k < 2 \times 10^{-15}$ m. The assumption of a sensitivity kept at

the standard quantum limit can be relaxed due to the short interaction time that limits the effect of the backaction. In principle, the sensitivity could even be increased by a factor close to $\langle n \rangle$, thus also making experiments with a larger $\langle n \rangle$ feasible. This can be accomplished, e.g., by increasing the measurement laser power. However, a major improvement is technically challenging, so we keep our previous conservative assumption.

So far we have considered the limits achievable by existing optomechanical experiments, but it is interesting to explore potential further advances. As we have shown, a small width of the ground-state position wave packet, and thus a large product $m\omega$, is a favorable characteristic for the purpose of reaching lower limits on l_k. In general, the larger the frequency is, the lower the mass is, although a larger $m\omega$ is more easily achieved in massive oscillators, where the relatively low frequency is more than offset by the large modal mass. However, experiments with low-frequency oscillators require lower temperatures to reach the quantum ground state, as well as higher sensitivities in position measurements due to the reduced x_{zpm}. In this context, resonant gravitational bar detectors represent the state-of-the-art, since they are designed to detect extremely small displacements and therefore exhibit very low background length fluctuations.

For instance, the first longitudinal mode of the AURIGA detector (a 2.3 ton aluminium bar with the first longitudinal mode oscillating at 1 kHz) has been cooled down to the milliKelvin regime using a cold damping technique [29]. Due to its large mass and relatively low temperature, it displays rms position fluctuations as low as $\sim 6 \times 10^{-19}$ m. The oscillator is in a thermal state, and it should be further cooled to an effective temperature five orders of magnitude smaller in order to approach the quantum ground state. Moreover, the detection system should be sensitive enough to measure the corresponding zero-point fluctuations at the level of $x_{\mathrm{zpm}} \sim 10^{-21}$ m, which is very far from being trivial to do. We thus turn our attention back to micro-oscillators that may enter the quantum regime in the near future.

For the purpose of this discussion we assume as reasonable experimental parameters a mechanical frequency $\omega/2\pi = 300$ kHz (at frequencies below 100 kHz acoustic and/or technical noise is usually too strong), a mechanical quality factor $Q = 10^7$, and a background displacement noise (i.e., the sensitivity) of 10^{-38} m^2/Hz. Starting from a base temperature of 0.1 K, the mechanical mode should be actively cooled to an effective quality factor $Q_{\mathrm{eff}} = 1500$ in order to reach a thermal occupancy $\langle n_{\mathrm{eff}} \rangle = 1$. In these conditions, setting the sensitivity as a lower limit to the final peak spectral density, we derive $m = 10^{-5}$ kg and thus $x_{\mathrm{zpm}} \simeq 2 \times 10^{-18}$ m. On the basis of these considerations, masses of around 10^{-5} kg represent a reasonable limit for the achievement and measurement of the quantum regime in mechanical resonators.

Optomechanical devices with similar characteristics have already been realized, though not yet cooled down to their quantum ground state. For instance, the literature reports silicon micromirrors with flexural-torsional modes oscillating at $\omega/2\pi = 100$–200 kHz, masses of $m = 2$–3×10^{-7} kg, and mechanical quality factors, measured at cryogenic temperatures, of $Q = 1$–3×10^6 [30,31] as well as quartz micropillars with a compression-dilatation mode at $\omega/2\pi = 3$–4 MHz, $m = 2$–4×10^{-8} kg, and $Q = 2.5 \times 10^7$ [32,33]. For all these devices, the zero-point fluctuations are of the order of $x_{\mathrm{zpm}} \simeq 10^{-2}$ fm. Operating at a background temperature of 100 mK, we have $\langle n \rangle \sim 600$ for the quartz oscillator and a reasonable upper limit for l_k of a few 10^{-18} m.

In summary, the bounds on the nonlocal scale obtainable with measurements on the ground state range from $l_k \leq 10^{-15}$ m to $l_k \leq 10^{-18}$ m. The latter is reasonably close to the constraint obtained at the LHC.

B. Evolution of coherent states

A further comparison between our theory and experiments can be based on the evolution of coherent states. As shown in Eq. (35), our model predicts a third-harmonic component in $\langle x \rangle$, with a ratio between third- and first-harmonic amplitudes (third-harmonic distortion, H_3) equal to $H_3 = \epsilon \alpha^2/8$. Using the definition of $\epsilon = l_k^2/(2x_{\mathrm{zpm}}^2)$, an upper limit to the nonlocal length can be set in the form $l_k < 4\sqrt{H_3}x_{\mathrm{zpm}}/\alpha$. The bound on l_k now also depends on $1/\alpha$ and can therefore be substantially lowered for high values of the coherent amplitude.

In order to prepare a quantum-coherent state, the system is first cooled down to its quantum ground state. As before, the measurement is then limited by the thermal decoherence time τ. We remark that, with an intracavity power P_{cav}, the oscillator is typically displaced from its equilibrium position, due to the radiation pressure, by $x_0 = (P_{\mathrm{cav}}/2c)/(m\omega^2)$. Once the cooling laser is turned off, this initial position determines a coherent state with amplitude $\alpha = x_0/\sqrt{2}x_{\mathrm{zpm}}$. The upper limit on the non-locality scale can thus be written as $l_k < 4\sqrt{2H_3}x_{\mathrm{zpm}}^2/x_0$, where x_0 is typically of the order of the cavity linewidth, i.e., ~ 10 pm. As a consequence, it is not obvious to further excite the oscillator while cooling. On the other hand, one can conceive a coherent excitation with optical power P_{exc} just after the cooling stage, during a time interval $T_{\mathrm{exc}} \ll \tau$, and reach a displacement $x_0 = T_{\mathrm{exc}} \times (P_{\mathrm{exc}}/2c)/2m\omega$.

Using a low-finesse optical cavity for this strong excitation pulse (this can be accomplished, e.g., by using the same cavity exploited for the optical cooling at a different wavelength), it is reasonable to achieve a x_0 of ~ 1–10 nm. The parameter H_3 could then be evaluated from the power spectral density of the signal monitoring the oscillator's position during a measurement period $\sim \tau$ following the excitation. We notice that a weak

measurement (maybe with an optical signal seeing the cavity at low finesse) is sufficient to detect a possible third-harmonic signal that must be compared with the main coherent component; i.e., a sensitivity close to the quantum limit is not necessary here.

For the SiN or aluminum membranes mentioned before ($x_{zpf} \simeq 1$ fm), one can aim to explore nonlocal scales down to $\sim 10^{-22}$ m. It is worth mentioning that an excitation yielding a coherent amplitude of several nanometers has already be applied to SiN membranes, and the experimental constraints on the third-harmonic distortion were similar to those that we are now considering [34]. The oscillator was in a thermal coherent state, but the results demonstrate that structural nonlinear effects are not a limit at this level. The use of the heavier oscillators discussed above could yield a further improvement of four orders of magnitude, to $\sim 10^{-26}$ m.

Besides the third-harmonic distortion, even the time-averaged variance is a useful indicator of possible nonlocal effects. To experimentally evaluate it one should first subtract, during the measurement period τ, the coherent component (whose two parameters, amplitude and phase, can be extracted either from the complete decay or from the average over consecutive realizations) from the signal measuring x. The signal must then be time averaged along the interval τ, and the mean square calculated over the result of repeated cycles.

Our model predicts that the effects of nonlocality on $\text{Var}(x)$ are enhanced with respect to the ground state by the coherent amplitude α. Taking the time average of Eq. (37) with $\alpha \gg 1$, we derive an upper limit to ϵ of the form $\epsilon < \Delta_{\text{meas}}/3\alpha^2$, and then $l_k < \sqrt{2\Delta_{\text{meas}}/3}\, x_{zpm}/\alpha$ or $l_k < \sqrt{4\Delta_{\text{meas}}/3}\, x_{zpm}^2/x_0$. The expected achievable limits on l_k are roughly the same as those discussed for the harmonic distortion, so the evaluation of both indicators would provide a useful cross-check. However, we remark that in this case the dynamic range and the accuracy in the subtraction of the coherent component is a critical issue and could reduce the potential measurement sensitivity.

VI. CONCLUSIONS AND DISCUSSION

We have shown that the nonrelativistic limit of an analytic nonlocal Klein-Gordon equation leads to a nonlocal generalization of the Schrödinger equation (7). We then constructed a phenomenological model in which the evolution of a single-particle wave function in a harmonic-oscillator potential is governed by such a nonlocal Schrödinger equation. This system is of particular interest to us because it is used to model the evolution of quantum optomechanical oscillators that are experimentally accessible. The introduction of the scale ω in the harmonic potential allowed us to construct a small dimensionless parameter $\epsilon = m\omega l_k^2/\hbar$, with which we defined a perturbative expansion of the nonlocal differential operator $f(\mathcal{S})$.

We showed that a perturbative analysis of the nonlocal system (24) leads to a sequence of ordinary Schrödinger equations, order by order in ϵ, with harmonic-oscillator potential and in the presence of a source term. At every order ϵ^n the source term was shown to depend on the solution to the problem at order ϵ^{n-1} for $n \geq 1$. We then solved the system of equations to first order in ϵ for perturbations around a coherent state by using the method of multiple scales. Having found that the resulting first-order wave function failed to immediately lead to a well-defined probability measure, we normalized it such that a consistent probability measure could be defined.

With this measure at hand we computed the expectation values and variances of observables x and p. We found that the expectation values are unaltered for perturbations around the ground state ($\alpha = 0$) but acquire a third harmonic for all $\alpha > 0$ (except for the peculiar case $\alpha = 1/\sqrt{6}$). Remarkably though, the state remains one of minimum uncertainty, i.e., $\text{Var}(x)\text{Var}(p) = 1/4 + O(\epsilon^2)$, for all α, while undergoing a spontaneous periodic time-dependent squeezing in phase space.

Finally, in Sec. V we discussed how the prediction of both of these effects can be used to test the model experimentally. In particular, we argued that, for the ground state, a comparison between the measured variance of x and existing optomechanical macroscopic oscillator experiments leads to bounds on l_k of the order of 10^{-15} m. By imagining reasonable near-future advances in these experiments, we further argued that bounds on l_k of the order of 10^{-18} m could be achieved. This last number would provide an independent bound on nonlocality of the order of the bound found using LHC data, with relatively inexpensive table-top experiments.

Extending the analysis to comparisons between these experiments and the predicted third harmonic component in $\langle x \rangle$, in Sec. V B we argued that bounds of the order of $l_k \sim 10^{-22}$ m can be achieved by looking at the evolution of coherent states. Improvements of four orders of magnitude are experimentally possible by using heavier oscillators, making constraints of order $l_k \sim 10^{-26}$ m possible in the near future. Similar bounds were then envisaged by making use of the oscillator's time-averaged variance, thus providing a potential cross-check of the previous analysis.

Note that the effects related to a third harmonic in the evolution of $\langle x \rangle$ can only be used to cast constraints on l_k since one can imagine similar effects being induced by the environment, and therefore only a lack of signal would be truly meaningful within this context. However, our model does provide a "smoking gun" of the nonlocal evolution, namely the time-dependent, periodic squeezing of the state in position and momenta, whose magnitude grows with the coherent amplitude α. Indeed, there exist no other effects that we are aware of that could lead to such a spontaneous squeezing. In order to detect this effect though, one should adopt a different operative scheme with respect to the one

discussed in Sec. V B. In particular, after the subtraction of the coherent component of the signal, one should not average over the whole measurement interval τ but over time bins much shorter (say, $1/10$) than the oscillation period. The mean square would then be calculated over results belonging to several consecutive cycles for the same time bins. The time-dependent variance would thus be reconstructed. The sensitivity to nonlocal effects is expected to be similar to the one analyzed for the time-averaged variance.

Finally, let us now elaborate on the theoretical improvements that could (and should) be made to further strengthen our analysis. The model we constructed is phenomenological in the sense that, although we were able to find a nonlocal Schrödinger equation for the nonrelativistic field ψ, we did not show that this field could be consistently taken to represent a one-particle quantum-mechanical wave function satisfying the nonlocal Schrödinger equation (7).

To fill this gap, one would need the Hamiltonian H_{NL} of the nonlocal system and use it to show that the one-particle wave function indeed satisfies the equation

$$i\hbar \frac{\partial \psi}{\partial t} = H_{NL}\psi, \tag{40}$$

where H_{NL} would also contain higher-order time derivatives. As well as providing a more direct link between the underlying nonlocal QFT and the nonrelativistic quantum system, a Hamiltonian formulation would also enable one to explicitly treat the oscillator as an open quantum system via a generalized kind of master equation. This description would allow for effects like decoherence and environmental noise to be taken into account, and it would be better apt for investigating the effects of nonlocality on the evolution of thermal coherent states, which are much easier to construct experimentally than pure coherent states and are therefore better suited to experimental comparison. It should also be noted that despite the fact that a preliminary analysis for thermal coherent states could be performed in the formalism laid out in this paper,[5] the Hamiltonian formalism would still be better suited for this given that thermal coherent states are mixed.

The Hamiltonian analysis aside, recall that our computation of expectation values of observables forced us to normalize the wave function with its own norm in order to define a sensible probability density. At the perturbative level one can check that the conserved charge (34) is *not* positive definite, but contains strongly suppressed negative regions. Thus, rigorously speaking, it cannot be interpreted as a probability density, something which points towards the fact that a positive definite charge can only be obtained

nonperturbatively. It is, however, possible to ignore these difficulties by using the charge, which is conserved to first order ϵ, in the computation of expectation values. When doing so, the results for the expectation values and variances are qualitatively similar to the ones shown in this work, and the phenomenologically relevant effect of spontaneous squeezing of coherent states persists.

To conclude, this analysis shows that optomechanical experiments have the potential to become a fundamental tool for high precision tests of quantum gravity-induced nonlocality. Although achieving Planck-scale sensitivities may not be strictly necessary in order to severely constrain certain quantum gravity scenarios, we believe that the rapid improvements of experimental techniques and instruments over recent years bode well for the possibility that this scale may be closely approached in the next decade or so. It appears, therefore, that a new branch of quantum gravity phenomenology is about to begin, and we hope that the present work will further stimulate such a turn of events.

APPENDIX: MULTIPLE SCALES METHOD

The method of multiple scales is needed for problems in which the solutions depend simultaneously on widely different scales. The method introduces one or more new slow-time variables for each time scale of interest in the problem and subsequently treats these variables as if they are independent. To ensure a valid approximation to the solutions of our perturbation problem, we can use a simple two-scale expansion as the nonlocal Schrödinger equation in dimensionless variables is characterized by the time evolution scale $\omega = 1$ and the nonlocality scale $\varepsilon \ll 1$. Here, the straightforward perturbative expansion in powers of ϵ leads to a nonuniform expansion where the perturbative ordering of the terms breaks down due to the presence of secular terms proportional to ϵt. The trick is to introduce a new variable $\hat{\tau} = \epsilon \hat{t}$, called the slow time because is not significant until $\hat{t} \sim 1/\epsilon$. Then, the solution of the nonlocal Schrödinger equation can be written as

$$\psi(\hat{t}, \hat{x}) = \psi_0(\hat{t}, \hat{\tau}, \hat{x}) + \epsilon\psi_1(\hat{t}, \hat{\tau}, \hat{x}) + \ldots. \tag{A1}$$

Using the chain rule, we have

$$\frac{d}{d\hat{t}}\psi = \frac{\partial}{\partial \hat{t}}\psi_0 + \epsilon\left(\frac{\partial}{\partial \hat{\tau}}\psi_0 + \frac{\partial}{\partial \hat{t}}\psi_1\right) + \ldots. \tag{A2}$$

---

[5]Recall that in the Glauber-Sudarshan *P*-representation the density matrix of a thermal coherent state is expressed in terms of pure coherent state projectors.

Substituting (A1) into equation (13), using (A2) and equating terms of order ϵ^0 and ϵ^1, gives

$$\left(\hat{S} - \frac{1}{2}\hat{x}^2\right)\psi_0 = 0, \tag{A3}$$

$$\left(\hat{S} - \frac{1}{2}\hat{x}^2\right)\psi_1 = 2a_2\hat{S}^2\psi_0 + \frac{\partial}{\partial\hat{\tau}}\psi_0. \tag{A4}$$

To ensure that there are no secular terms in our ansatz solution (27) for coherent states, the terms proportional to $\hat{t}$ in $\psi_1(\hat{t}, \hat{x})$ are forced to be 0 by assuming

$$\psi_0(\hat{t}, \hat{\tau}, \hat{x}) = \psi_0(\hat{t}, \hat{x})\exp[\hat{\tau}f(\hat{t}, \hat{x})\hat{t}], \tag{A5}$$

where $f(\hat{t}, \hat{x})$ is a suitable polynomial in $\hat{x}$ with time-dependent coefficients. To confirm the reliability of our solution method in Sec. IV, we have checked that there are no solutions growing in time as fast as $\epsilon\hat{t}$ by numerically solving the nonlocal Schrödinger equation. To this end, we solved the equation

$$(\hat{S} - 2a_2\epsilon\hat{S}^2 - \hat{x}^2/2)\psi(\hat{t}, \hat{x}) = 0$$

in the rectangular domain $[-6 \leq x \leq 6] \times [0 \leq t \leq 25]$ of the spacetime plane, with $2a_2\epsilon = 10^{-3}$ and periodic boundary conditions in space. In addition, we set the initial conditions

$$\psi(0, \hat{x}) = \frac{1}{\pi^{1/4}}\exp\left[\sqrt{2}\hat{x} - \frac{\hat{x}^2}{2} - 1\right]$$

$$\frac{d}{d\hat{t}}\psi(\hat{t}, \hat{x})\Big|_{\hat{t}=0} = -\frac{ie^{-\frac{\hat{x}^2}{2}+\sqrt{2}\hat{x}-1}(2\sqrt{2}\hat{x}-1)}{2\pi^{1/4}},$$

representing the $\alpha = 1$ coherent state. The numerical solution was calculated using the implicit Euler method of the partial differential equation solver provided by MATHEMATICA. To quantify numerical errors in the discrete space and time domains, we introduce the Chebyshev distance between solutions ψ_1 and ψ_2 as
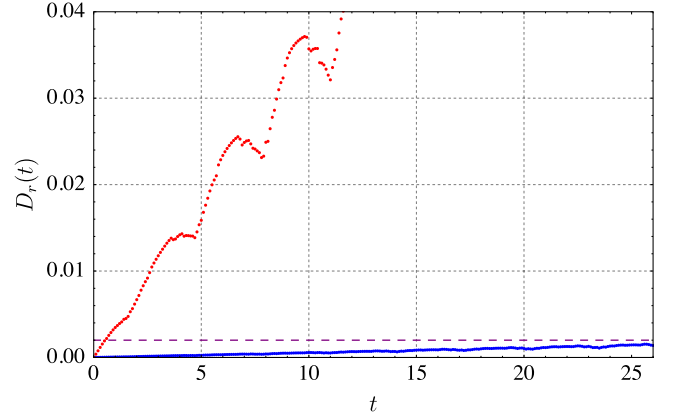

FIG. 4. Time dependence of the relative distance $D_r(\hat{t}_k) \equiv D(\hat{t}_k)/\max_j\{|\psi(\hat{t}_k, \hat{x}_j)|\}$ among perturbed solutions of the non-local Schrödinger equation. For the numerical solution, we fix $\alpha = 1$ and $a_2\epsilon = 2 \times 10^{-3}$. The horizontal purple line is the relative distance threshold 2×10^{-3}. Blue dots represent the relative distance between numerical and analytical solutions. Red dots represent the relative distance between numerical and analytical solutions without dropping secular terms.

$$D(\hat{t}_k) \equiv \max_j\{|\psi_1(\hat{t}_k, \hat{x}_j) - \psi_2(\hat{t}_k, \hat{x}_j)|\}. \tag{A6}$$

To calculate $D(\hat{t}_k)$, we set the space mesh size to 10^{-2} and the time mesh size to 10^{-1}.

Figure 4 shows the plots of the relative maximum distances between the numerical and analytical solutions either removing or keeping terms $\epsilon\hat{t}$. These plots clearly show that secular terms in the polynomial coefficients $c_0(\hat{t}), c_1(\hat{t}), c_2(\hat{t}), c_3(\hat{t})$, and $c_4(\hat{t})$ of ψ_1 have been properly discarded. We stress that the small mismatch in Fig. 4 between numerical and analytical solutions is due to the accumulation of numerical errors at large time, as it does not grow as fast as $\epsilon\hat{t}$. As a final remark, we also point out that there is good agreement between mean and variance of position and momentum in Eqs. (35)–(38) evaluated with $\alpha = 1$, $2a_2\epsilon = 10^{-3}$, and the same quantities estimated by means of the numerical solution.

[1] N. Mavromatos, in *Planck Scale Effects in Astrophysics and Cosmology*, edited by G. Amelino-Camelia and J. Kowalski-Glikman (Springer-Verlag, Berlin, 2005), p. 245.

[2] S. Weinberg, Phys. Rev. D **72**, 043514 (2005).

[3] T. Damour and A. M. Polyakov, Nucl. Phys. **B423**, 532 (1994).

[4] J. D. Barrow, in International School of Astrophysics, D. Chalonge: 6th Course: Current Topics in Astrofundamental Physics: Primordial Cosmology Erice, Italy,

September 4-15, 1997 (1997), https://arxiv.org/pdf/gr-qc/9711084.pdf.

[5] M. Bleicher, S. Hofmann, S. Hossenfelder, and H. Stöcker, Phys. Lett. B **548**, 73 (2002).

[6] G. Amelino-Camelia, Nature (London) **398**, 216 (1999).

[7] L. J. Garay, Int. J. Mod. Phys. A **10**, 145 (1995).

[8] S. Hossenfelder, Living Rev. Relativ. **16**, 2 (2013).

[9] F. Marin, F. Marino, M. Bonaldi, M. Cerdonio, L. Conti, P. Falferi, R. Mezzena, A. Ortolan, G. A. Prodi, L. Taffarello,

G. Vedovato, A. Vinante, and J.-P. Zendri, Nat. Phys. **9**, 71 (2013).

[10] V. A. Kostelecky, Phys. Rev. D **69**, 105009 (2004).

[11] D. Mattingly, Living Rev. Relativ. **8**, 5 (2005).

[12] S. Liberati, Classical Quantum Gravity **30**, 133001 (2013).

[13] R. D. Sorkin, in *Approaches to Quantum Gravity: Towards a New Understanding of Space and Time*, edited by D. Oriti (Cambridge University Press, Cambridge, England, 2006).

[14] D. A. Eliezer and R. P. Woodard, Nucl. Phys. **B325**, 389 (1989).

[15] R. J. Szabo, Phys. Rep. **378**, 207 (2003).

[16] R. Gambini and J. Pullin, Int. J. Mod. Phys. D **23**, 1442023 (2014).

[17] M. Ostrogradski, Petersbourg **1**, 18502 (1850).

[18] A. S. Koshelev, Rom. J. Phys. **57**, 894 (2012); see also G. Calcagni and L. Modesto Phys. Rev. D **91**, 124059 (2015) and references therein.

[19] A. Belenchia, D. M. T. Benincasa, and S. Liberati, J. High Energy Phys. 03 (2015) 036.

[20] A. Belenchia, D. M. T. Benincasa, E. Martin-Martinez, and M. Saravani, Phys. Rev. D **94**, 061902 (2016).

[21] A. Belenchia, D. M. T. Benincasa, S. Liberati, F. Marin, F. Marino, and A. Ortolan, Phys. Rev. Lett. **116**, 161303 (2016).

[22] D. Tong, Part III Cambridge University Mathematics Tripos, Michaelmas (2006), http://www.damtp.cam.ac.uk/user/tong/qft.html.

[23] C. Bollini and J. Giambiagi, Rev. Bras. Fis. **17**, 14 (1987).

[24] T. Biswas and N. Okada, Nucl. Phys. **B898**, 113 (2015).

[25] S. M. Meenehan, J. D. Cohen, G. S. MacCabe, F. Marsili, M. D. Shaw, and O. Painter, Phys. Rev. X **5**, 041002 (2015).

[26] R. Riedinger, S. Hong, R. A. Norte, J. A. Slater, J. Shang, A. G. Krause, V. Anant, M. Aspelmeyer, and S. Gröblacher, Nature (London) **530**, 313 (2016).

[27] F. Lecocq, J. B. Clark, R. W. Simmonds, J. Aumentado, and J. D. Teufel, Phys. Rev. X **5**, 041037 (2015).

[28] R. W. Peterson, T. P. Purdy, N. S. Kampel, R. W. Andrews, P.-L. Yu, K. W. Lehnert, and C. A. Regal, Phys. Rev. Lett. **116**, 063601 (2016).

[29] A. Vinante, M. Bignotto, M. Bonaldi, M. Cerdonio, L. Conti, P. Falferi, N. Liguori, S. Longo, R. Mezzena, A. Ortolan *et al.*, Phys. Rev. Lett. **101**, 033601 (2008).

[30] E. Serra, A. Borrielli, F. S. Cataliotti, F. Marin, F. Marino, A. Pontin, G. A. Prodi, and M. Bonaldi, Phys. Rev. A **86**, 051801 (2012).

[31] A. Borrielli, A. Pontin, F. S. Cataliotti, L. Marconi, F. Marin, F. Marino, G. Pandraud, G. A. Prodi, E. Serra, and M. Bonaldi, Phys. Rev. Applied **3**, 054009 (2015).

[32] A. G. Kuhn, M. Bahriz, O. Ducloux, C. Chartier, O. Le Traon, T. Briant, P.-F. Cohadon, A. Heidmann, C. Michel, L. Pinard, and R. Flaminio, Appl. Phys. Lett. **99**, 121103 (2011).

[33] L. Neuhaus *et al.*, in *Proceedings of JMC15*, Bordeaux, France, 2016, https://jmc15.sciencesconf.org/106353.

[34] M. Bawaj *et al.*, Nat. Commun. **6**, 7503 (2015).